

Theory status of hadronic top-quark pair production

Christian Schwinn ^a

*Institut für Theoretische Teilchenphysik und Kosmologie,
RWTH Aachen University, Sommerfeldstraße 16, D-52056 Aachen, Germany*

The status of theoretical predictions for top-quark pair production at hadron colliders is reviewed, focusing on the total cross section, differential distributions, and the description of top-quark production and decay including off-shell effects.

1 Introduction

The increasingly precise measurements of top-quark observables at the LHC require corresponding progress in their theoretical description. This contribution provides an overview of recent theory developments, from corrections beyond next-to-next-to-leading order (NNLO) for the total cross section in Section 2, via state-of-the-art combinations of NNLO QCD and NLO electroweak corrections for differential observables for stable tops in Section 3, to descriptions of the full production and decay process and the effects on the m_t measurement in Section 4.

2 Total cross section

The total top-quark pair production cross section provides an important benchmark measurement at the Tevatron and LHC that allows to measure the top mass in a well-defined scheme with an accuracy of 2 GeV,^{1,2} and to determine the strong coupling constant α_s with an accuracy competitive with other determinations.^{3,4} A comparison of the NNLO QCD prediction⁵ for different PDF sets^{6,7,8,9} to the most precise experimental LHC results at $\sqrt{s} = 13$ TeV¹⁰ in Figure 1 shows good agreement among the PDF sets^b and with the experimental results, whose precision challenge that of the NNLO calculation. Since a full N³LO calculation is currently out of reach, attempts to reduce the perturbative uncertainties further rely on resummation methods to compute higher-order corrections enhanced in certain kinematic limits. For the total partonic cross section, corrections enhanced in the partonic threshold limit $\beta = \sqrt{1 - 4m_t^2/\hat{s}} \rightarrow 0$ are given by logarithmic soft-gluon corrections, $\alpha_s \ln^2 \beta$, and Coulomb corrections, α_s/β . The logarithmic accuracy of the resummed cross section can be defined in a “primed” and “unprimed” counting, depending on the inclusion of fixed-order non-logarithmic corrections:

$$\hat{\sigma} \propto \hat{\sigma}^{(0)} \sum_{k=0} \left(\frac{\alpha_s}{\beta} \right)^k \exp \left[\underbrace{\ln \beta g_0(\alpha_s \ln \beta)}_{(\text{LL})} + \underbrace{g_1(\alpha_s \ln \beta)}_{(\text{NLL})} + \underbrace{\alpha_s g_2(\alpha_s \ln \beta)}_{(\text{NNLL})} + \underbrace{\alpha_s^2 g_3(\alpha_s \ln \beta)}_{(\text{N}^3\text{LL})} + \dots \right] \times \left\{ 1 (\text{LL}, \text{NLL}); \alpha_s, \beta (\text{NLL}', \text{NNLL}); \alpha_s^2, \alpha_s \beta, \beta^2 (\text{NNLL}', \text{N}^3\text{LL}); \dots \right\}. \quad (1)$$

^aSupported by the Heisenberg Programme of the DFG

^b For ABMP16⁹ the values for $\alpha_s(M_Z)$ and m_t preferred by the PDF fit have been employed. Note that in this set as well as in MMHT14⁶ and NNPDF3.1⁸ LHC data on $t\bar{t}$ production are already used in the fit.

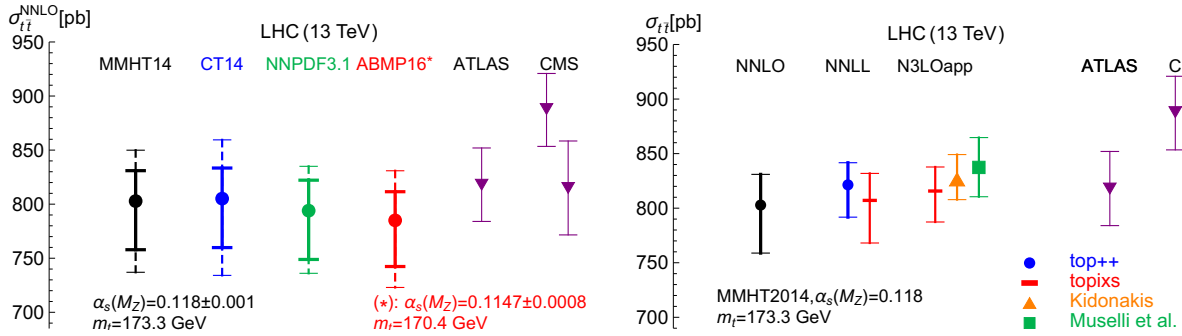


Figure 1 – Left: Comparison of the total $t\bar{t}$ cross section at NNLO QCD with different PDFs to LHC measurements at 13 TeV including the scale uncertainty (solid lines) and the 68% confidence-level PDF+ α_s uncertainty (dashed lines). Right: Different predictions of higher-order threshold corrections. For **topixs** and Muselli et al. the scale uncertainty is added in quadrature to the systematic uncertainty of the threshold approximation. The relative corrections of Muselli et al. and Kidonakis have been rescaled by the NNLO result with MMHT2014 PDFs.

In Figure 1 the **top++** 2.0¹¹ result for NNLL soft-gluon resummation in Mellin space¹² is compared to the combined soft/Coulomb-gluon resummation in momentum space¹³ implemented in **topixs**.¹⁴ The main numerical difference is due¹⁵ to an NNLL' effect from $\mathcal{O}(\alpha_s^2)$ constants included in **top++**, while the Coulomb corrections included in **topixs** have a smaller effect.

As an alternative to all-order resummation, approximate N³LO results have been computed using different resummation methods and logarithmic accuracy. The calculation of Kidonakis¹⁶ is based on NNLL resummation for one-particle inclusive kinematics. Muselli et al.¹⁷ use partial N³LL soft resummation in Mellin space, including $1/N$ -suppressed contributions and information on the large- β behaviour. A calculation based on partial N³LL soft resummation and N³LO Coulomb corrections¹⁵ is implemented in **topixs3.0**. All N³LO_{app} predictions are consistent with the resummed NNLL calculations and have a similar scale uncertainty of $\pm 3\%$, which suggests that corrections beyond N³LO are indeed small. The range of the different implementations of higher-order threshold corrections, which include complementary effects, indicates that the scale uncertainty underestimates the true perturbative uncertainty and should be supplemented by an 1–2% estimate of systematic uncertainties^{13,17,15} due to the threshold approximation.

3 Differential distributions

With the increase of the LHC centre-of-mass energy to 13 TeV and accumulating luminosity, the measurement of observables such as transverse-momentum or invariant-mass distributions in the TeV range becomes increasingly precise and requires matching theoretical predictions. The theoretical description of such differential distribution has recently been achieved at NNLO accuracy in QCD.¹⁸ As an application of differential NNLO predictions, it has been advocated to constrain the gluon PDF using rapidity distributions,¹⁹ which are argued to be robust against variations of the top mass and possible new-physics effects. For specific observables, fixed-order calculations can be complemented by NNLL resummation in various kinematic regimes such as the low p_T limit.^{20,21} NNLL resummation for boosted tops,²² which simultaneously resums threshold logarithms in the pair-invariant mass, $\ln(1 - M_{t\bar{t}}^2/\hat{s})$, and mass logarithms $\ln(m_t^2/\hat{s})$, has allowed to validate dynamical scale choices $\mu_f = H_T/4 = \frac{1}{4}(\sqrt{m_t^2 + p_{T,t}^2} + \sqrt{m_t^2 + p_{T,\bar{t}}^2})$ for the $M_{t\bar{t}}$ spectrum and $\mu_f = m_T/2$ for the p_t spectrum.²³

At high p_T , both higher order QCD corrections and EW corrections, which are dominated by Sudakov effects, are necessary for a proper theoretical description. A multiplicative combination of NNLO QCD and NLO EW corrections²⁴ is advocated to capture the dominant higher-order soft-QCD/EW-Sudakov effects at large p_T . In a complementary work,²⁵ the interplay of real-gluon emission and EW corrections is modeled using parton-shower merging of the processes

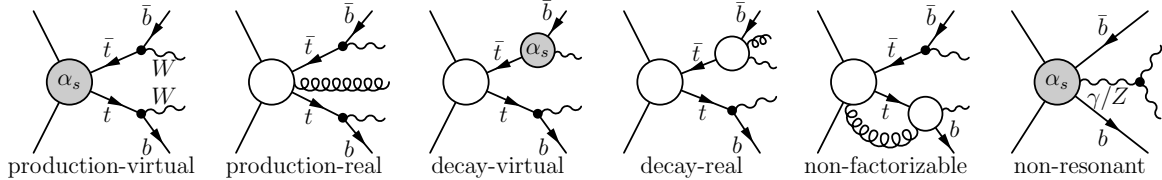


Figure 2 – Example topologies of diagrams for the process $pp \rightarrow b\bar{b}W^+W^-$ arising in the narrow-width approximation, the double-pole approximation, and the full off-shell NLO QCD calculation for unstable top quarks. The decay products of the W bosons are not shown.

$t\bar{t}$ and $t\bar{t}j$ at NLO QCD+EW_{virt} accuracy. Here the NLO EW corrections are included in a virtual approximation supplemented with real photonic corrections in the YFS approximation. The results of these works show that the EW corrections become relevant for the comparison to experimental data for $p_T > 500$ GeV.

4 Top-quark production and decay

Kinematic observables entering studies of top-quark properties such as spin correlations or the ”direct” measurement of the top-quark mass require to go beyond the approximation of stable top quarks and include the top decay products. Since the decay width of the top quark is relatively small, $\Gamma_t/m_t \sim 1\%$, in generic kinematic situations the narrow-width approximation (NWA) of the production cross section of the resulting $b\bar{b} + 4f$ -final state may be performed,

$$\sigma_{pp \rightarrow b\bar{b}4f} \Rightarrow \sigma_{pp \rightarrow t\bar{t}} \times \frac{\Gamma_{t \rightarrow bf_1f_2}}{\Gamma_t} \frac{\Gamma_{\bar{t} \rightarrow \bar{b}f_3f_4}}{\Gamma_t}. \quad (2)$$

In the framework of the NWA, spin correlations and QCD^{26,27} as well as EW corrections²⁸ can be incorporated, including real and virtual corrections to the production and decay of on-shell tops. In a step beyond the NWA, the double-pole approximation additionally includes Breit-Wigner propagators and non-factorizable corrections connecting initial and final states.²⁹ NLO computations for the full $pp \rightarrow b\bar{b} + 4f$ processes further include full off-shell effects and non-resonant contributions. Here NLO QCD corrections for the di-lepton $pp \rightarrow b\bar{b}l\nu_\ell l'\nu_{\ell'}$ ^{30,31} and semileptonic final state $pp \rightarrow b\bar{b}l\nu_\ell jj$,³² as well as EW corrections for the di-lepton final state³³ are available. Example NLO QCD topologies for the different contributions are shown in Figure 2. A description of top production and decay at NNLO is currently only feasible in the NWA, where an approximate differential NNLO calculation of top-quark production³⁴ has been combined³⁵ with the NNLO decay corrections.^{36,37} Recently also preliminary results using the exact NNLO production cross section have been presented.³⁸ These calculations show promise for an improved description of experimental results on spin correlations.

Comparisons of the NWA and fully off-shell NLO QCD calculations^{39,40} show the expected accuracy of $\mathcal{O}(\Gamma_t/m_t)$ for generic kinematics, provided NLO decay corrections are included, which can reach a size of 20%. Above kinematic edges, for instance above the invariant mass $m_{\ell b} = \sqrt{m_t^2 - M_W^2}$, nonresonant contributions dominate and the NWA fails. The effect of off-shell effects on the extraction of the top mass has been studied comparing the NWA to full off-shell calculations. Performing a template fit of the $m_{\ell b}$ distribution using partonic cross sections, a sizable shift of 0.8 GeV due to off-shell effects was reported.⁴⁰ From the shift of the peak position of the $m_{\ell b}$ distribution and using off-shell NLO calculations matched to a resonance-aware parton shower,⁴² a more moderate effect of ~ 0.1 GeV was found.⁴¹ However, larger effects were found for the Herwig shower than for Pythia. Both studies do not fully correspond to the experimental situation so further work is needed for conclusive statements. In addition, other effects relevant for the interpretation of the top-mass measurements at hadron colliders such as renormalon effects on the relation of the pole-mass to short-distance mass definitions⁴³ or the impact of parton-shower effects on the mass definition⁴⁴ remain controversial.

References

1. ATLAS, G. Aad et al., Eur. Phys. J. C74 (2014) 3109, arXiv:1406.5375, [Addendum: Eur. Phys. J. C76, no.11, 642 (2016)].
2. CMS, V. Khachatryan et al., JHEP 08 (2016) 029, arXiv:1603.02303.
3. T. Klijnsma et al., Eur. Phys. J. C77 (2017) 778, arXiv:1708.07495;
4. CMS, S. Chatrchyan et al., Phys. Lett. B728 (2014) 496, arXiv:1307.1907, [Erratum: Phys. Lett. B738, 526 (2014)].
5. M. Czakon, P. Fiedler and A. Mitov, Phys. Rev. Lett. 110 (2013) 252004, arXiv:1303.6254.
6. L. Harland-Lang et al., Eur. Phys. J. C75 (2015) 204, arXiv:1412.3989.
7. S. Dulat et al., Phys. Rev. D93 (2016) 033006, arXiv:1506.07443.
8. NNPDF, R.D. Ball et al., Eur. Phys. J. C77 (2017) 663, arXiv:1706.00428.
9. S. Alekhin et al., Phys. Rev. D96 (2017) 014011, arXiv:1701.05838.
10. ATLAS, M. Aaboud et al., Phys. Lett. B761 (2016) 136, arXiv:1606.02699, [Erratum: Phys. Lett. B772, 879 (2017)]; CMS, V. Khachatryan et al., Eur. Phys. J. C77 (2017) 172, arXiv:1611.04040; CMS, A.M. Sirunyan et al., JHEP 09 (2017) 051, arXiv:1701.06228.
11. M. Czakon and A. Mitov, Comput. Phys. Commun. 185 (2014) 2930, arXiv:1112.5675.
12. M. Cacciari et al., Phys. Lett. B710 (2012) 612, arXiv:1111.5869.
13. M. Beneke et al., Nucl. Phys. B855 (2012) 695, arXiv:1109.1536.
14. M. Beneke et al., JHEP 1207 (2012) 194, arXiv:1206.2454.
15. J. Piclum and C. Schwinn, JHEP 03 (2018) 164, arXiv:1801.05788.
16. N. Kidonakis, Phys. Rev. D90 (2014) 014006, arXiv:1405.7046.
17. C. Muselli et al., JHEP 08 (2015) 076, arXiv:1505.02006.
18. M. Czakon et al., JHEP 05 (2016) 034, arXiv:1601.05375.
19. M. Czakon et al., JHEP 04 (2017) 044, arXiv:1611.08609.
20. H.T. Li et al., Phys. Rev. D88 (2013) 074004, arXiv:1307.2464.
21. S. Catani, M. Grazzini and H. Sargsyan, (2018), arXiv:1806.01601.
22. B.D. Pecjak et al., Phys. Rev. Lett. 116 (2016) 202001, arXiv:1601.07020.
23. M. Czakon et al., JHEP 05 (2018) 149, arXiv:1803.07623.
24. M. Czakon et al., JHEP 10 (2017) 186, arXiv:1705.04105.
25. C. Gütschow et al., Eur. Phys. J. C78 (2018) 317, arXiv:1803.00950.
26. W. Bernreuther et al., Nucl. Phys. B690 (2004) 81, arXiv:hep-ph/0403035.
27. K. Melnikov and M. Schulze, JHEP 08 (2009) 049, arXiv:0907.3090.
28. W. Bernreuther and Z.G. Si, Nucl. Phys. B837 (2010) 90, arXiv:1003.3926.
29. P. Falgari, A.S. Papanastasiou and A. Signer, JHEP 05 (2013) 156, arXiv:1303.5299.
30. A. Denner et al., Phys. Rev. Lett. 106 (2011) 052001, arXiv:1012.3975.
31. G. Bevilacqua et al., JHEP 02 (2011) 083, arXiv:1012.4230.
32. A. Denner and M. Pellen, JHEP 02 (2018) 013, arXiv:1711.10359.
33. A. Denner and M. Pellen, JHEP 08 (2016) 155, arXiv:1607.05571.
34. A. Broggio, A.S. Papanastasiou and A. Signer, JHEP 10 (2014) 98, arXiv:1407.2532.
35. J. Gao and A.S. Papanastasiou, Phys. Rev. D96 (2017) 051501, arXiv:1705.08903.
36. J. Gao, C.S. Li and H.X. Zhu, Phys. Rev. Lett. 110 (2013) 042001, arXiv:1210.2808.
37. M. Brucherseifer, F. Caola and K. Melnikov, JHEP 04 (2013) 059, arXiv:1301.7133.
38. R. Poncelet, Talk presented at Top2018, 16-21 September 2018 Bad Neuenahr, Germany.
39. J. Alcaraz Maestre et al., 7th Les Houches Workshop on Physics at TeV Colliders, arXiv:1203.6803.
40. G. Heinrich et al., JHEP 07 (2018) 129, arXiv:1709.08615.
41. S. Ferrario Ravasio et al., Eur. Phys. J. C78 (2018) 458, arXiv:1801.03944.
42. T. Ježo et al., Eur. Phys. J. C76 (2016) 691, arXiv:1607.04538.
43. See e.g. P. Nason, (2017), arXiv:1712.02796 and references therein.
44. A.H. Hoang, S. Plätzer and D. Samitz, (2018), arXiv:1807.06617.